

Published in final edited form as:

Circulation. 2009 March 10; 119(9): 1241–1252. doi:10.1161/CIRCULATIONAHA.108.783852.

Chronic Cardiac-Targeted RNA Interference for the Treatment of Heart Failure Restores Cardiac Function and Reduces Pathological Hypertrophy

Lennart Suckau, BSc¹, Henry Fechner, DVM¹, Elie Chemaly, MD², Stefanie Krohn, BSc¹, Lahouaria Hadri, PhD², Jens Kockskämper, MD³, Dirk Westermann, MD¹, Egbert Bisping, MD³, Hung Ly, MD², Xiaomin Wang, BSc¹, Yoshiaki Kawase, MD², Jiqui Chen, MD², Lifan Liang, MD², Isaac Sipo, PhD¹, Roland Vetter, MD⁴, Stefan Weger, PhD⁵, Jens Kurreck, PhD⁶, Volker Erdmann, PhD⁶, Carsten Tschope, MD¹, Burkert Pieske, MD³, Djamel Lebeche, PhD², Heinz-Peter Schultheiss, MD¹, Roger J. Hajjar, MD^{1,2}, and Wolfgang Ch. Poller, MD^{1,1,§}

¹Dept. of Cardiology & Pneumology, Campus *Benjamin Franklin*, Charité - Universitätsmedizin Berlin, 12200 Berlin, Germany.

²Cardiovascular Research Center, Mt. Sinai School of Medicine, New York, NY 10029, USA.

³Dept. of Cardiology, Medical University of Graz, 8036 Graz, Austria.

⁴Dept. of Pharmacology & Toxicology, Campus *Benjamin Franklin*, Charité - Universitätsmedizin Berlin, 12200 Berlin, Germany.

⁵Dept. of Virology, Campus *Benjamin Franklin*, Charité - Universitätsmedizin Berlin, 12200 Berlin, Germany.

⁶Institute of Biochemistry, Freie Universität Berlin, 14192 Berlin, Germany.

Abstract

Background—RNA interference (RNAi) has the potential to be a novel therapeutic strategy in diverse areas of medicine. We report on targeted RNAi for the treatment of heart failure (HF), an important disorder in humans resulting from multiple etiologies. Successful treatment of HF is demonstrated in a rat model of transaortic banding by RNAi targeting of phospholamban (PLB), a key regulator of cardiac Ca²⁺ homeostasis. Whereas gene therapy rests on recombinant protein expression as its basic principle, RNAi therapy employs regulatory RNAs to achieve its effect.

Methods and Results—We describe structural requirements to obtain high RNAi activity from adenoviral (AdV) and adeno-associated virus (AAV9) vectors and show that an AdV *short hairpin* RNA vector (AdV-shRNA) silenced PLB in cardiomyocytes (NRCMs) and improved hemodynamics in HF rats 1 month after aortic root injection. For simplified long-term therapy we

[§]To whom correspondence should be addressed. Prof. Wolfgang Poller, M.D. Department of Cardiology & Pneumology Campus *Benjamin Franklin* Charité - University Medicine Berlin Hindenburgdamm 30 D-12200 Berlin, Germany wolfgang.poller@charite.de.

[¶]These authors contributed equally.

AUTHOR CONTRIBUTIONS WP, RH, HF and LS designed and performed research, analyzed data, and wrote the paper. The other authors performed research or contributed analytical tools.

DISCLOSURES None.

developed a dimeric cardiotropic AAV vector (rAAV9-shPLB) delivering RNAi activity to the heart *via* intravenous injection. Cardiac PLB protein was reduced to 25% and SERCA2a suppression in the HF groups was rescued. In contrast to traditional vectors rAAV9 shows high affinity for myocardium, but low affinity for liver and other organs. rAAV9-shPLB therapy restored diastolic (LVEDP, dp/dt_{min} , Tau) and systolic (fractional shortening) functional parameters to normal range. The massive cardiac dilation was normalized and the cardiac hypertrophy, cardiomyocyte diameter and cardiac fibrosis significantly reduced. Importantly, there was no evidence of microRNA deregulation or hepatotoxicity during these RNAi therapies.

Conclusion—Our data show, for the first time, high efficacy of an RNAi therapeutic strategy in a cardiac disease.

Keywords

Heart Failure; RNA Interference; Gene Therapy; Adeno-Associated Virus; Phospholamban

INTRODUCTION

RNAi has been investigated as a new treatment option in infectious diseases and cancer. We report here on a strategy for the treatment of a cardiac disease by locally induced RNAi. HF remains a leading cause of mortality in the developed world. Current drug treatment has limited efficacy and in advanced HF left-ventricular assist devices or heart transplantation are ultimate options. For long-term treatment of HF novel approaches are being currently explored including gene and cell therapies, whereas RNAi to modulate cardiac gene functions has not yet been evaluated. Whereas gene therapy rests on recombinant protein expression as its basic principle, RNAi therapy employs instead small regulatory RNAs to achieve its effect. Targeting, kinetics, and toxicity of these RNAs *in vivo* are grossly different from those of recombinant proteins and not yet well characterized. Although HF may result from multiple etiologies, defective cardiac Ca^{2+} homeostasis has been identified as an important final common pathway. In this study, we show successful treatment of HF by RNAi targeting a key regulator of cardiac Ca^{2+} homeostasis. Malfunction of the failing heart is in part due to dysfunction of the PLB-controlled sarcoplasmic reticulum Ca^{2+} ATPase pump (SERCA2a) resulting from reduced SERCA2a expression and/or PLB phosphorylation 1. Unphosphorylated PLB keeps the Ca^{2+} affinity of SERCA2a low, resulting in decreased SR Ca^{2+} uptake, slowed relaxation and decreased SR Ca^{2+} load, while PLB phosphorylation in response to β -adrenergic stimulation relieves this inhibition 2. Germline ablation of the PLB gene, gene transfer for dominant negative PLB mutants 3,4, PLB-*antisense*-RNAs 5, and intracellular inhibitory PLB antibodies 6, 7 have been employed to increase SERCA2a activity and to rescue heart failure models 8. RNAi mediated by chemically synthesized *short interfering* RNAs (siRNAs) in cardiomyocytes showed very low efficacy and stability even *in vitro* 9 and pharmacological approaches at PLB modulation have failed so far. Fundamental limitations of synthetic siRNAs are their rapid degradation in plasma and target cells, and the unsolved problem of achieving adequate transfer and targeting *in vivo*. Viral vectors have the potential to overcome these limitations and we previously showed highly efficient PLB ablation in primary NRCMs by an adenoviral RNAi vector 10. No change in the expression of other cardiac proteins

including Ca^{2+} handling proteins occurred indicating high target specificity. In the present study we evaluated the principle of RNAi against PLB for acute and chronic treatment of HF *in vivo*. Functional characterization of a series of vectors and the determinants of their efficacy was followed by investigation of an optimized rAAV9 alongside a traditional adenoviral vector in an animal model of HF, and of cardiomyocyte microRNAs (miRNAs) during RNAi therapy.

METHODS

Development of Recombinant Adenoviral and AAV Vectors

Recombinant Adeno-Associated Virus (rAAV) vectors were developed for the *in vitro* studies as pseudotyped rAAV6 and for the *in vivo* work as rAAV9. Throughout all *in vitro* and *in vivo* studies we used only self-complementary AAV genomes due to their enhanced performance compared to single-stranded AAV vectors. Vector maps are shown in Fig. 1a. For the details of all methods see Online Supplement.

Vector Production and Purification, Quality Assessment and Titration

rAAV9-shGFP and rAAV9-shPLB were produced using a two-plasmids protocol described previously 11 with the following modifications. 293-T cells were grown in triple flasks for 24 h (DMEM, 10% FBS) prior to adding the calcium phosphate precipitate. After 72 hours, the virus was purified from benzonase-treated cell crude lysates over an iodixanol density gradient, followed by heparin-agarose type I affinity chromatography. Finally viruses were concentrated and formulated into lactated Ringer's solution using a Vivaspin 20 Centrifugal concentrators 50K MWCO, and stored at -80°C . Vector stock biochemical purity (>95%) was assessed by silver staining after electrophoresis. Genome containing particles were determined by real-time PCR approach.

Vector Evaluation in Primary Cardiomyocytes

Primary neonatal cardiomyocytes (NRCMs) are suitable to pre-test any RNAi-based cardiac therapy before its definitive test *in vivo* since, although developmentally regulated, the SERCA2a/PLB system functions well in NRCMs and adenoviral gene transfer strategies targeting the SERCA2a/PLB system were successful in both neonatal and adult cardiomyocytes. Although both cell types are suited for *in vitro* pre-testing, a number of other differences between cultured cardiomyocytes and the intact heart *in vivo* render any *in vitro* study of RNA-based therapies in cultured cells preliminary. *Cell cultures*: NRCMs were prepared from ventricular tissue of 1-3 days-old Wistar rat pups and grown in 6-well dishes. *Evaluation of PLB silencing*: PLB, TnI, NCX, and SERCA2a mRNA or protein expression were determined by Northern and Western blot analyses as described previously 10. *Calcium Transients During RNAi Treatment*: $[\text{Ca}^{2+}]_i$ transients were measured during electrical stimulation at 1 Hz after loading of NRCMs with $8\ \mu\text{M}$ Fluo-4/AM for 20 min (image capture at 120 Hz, 8.3 ms per image). Five treatment groups of NRCMs (number of cells) were studied: AAV9-shPLB (n=26), AAV9-shGFP (n=26), AdV-shPLB (n=71), AdV-shGFP (n=49), and untreated control cells (n=32). The amplitude of the transient (systolic $[\text{Ca}^{2+}]$ (F/F_0)), its time to peak (TTP) (ms), and the time constant τ of its decay (ms) were measured.

Induction of hypertrophy: Phenylephrine (PE) at a concentration of 100 μM was employed in part of the *in vitro* studies as a hypertrophic stimulus. TaqMan assays to quantitate the cellular miRNAs were performed in NRCMs under baseline conditions or in the presence of PE, or in rat hearts. The agent was added on day 2 of culture, either alone or together with the respective RNAi vector. *miRNA assays:* In search for possible influences of vector-derived shRNAs on cardiomyocyte miRNAs we used *TaqMan* assays to quantitate two miRNAs with known cardiac functions 12-16.

Transaortic Banding and Serial Echocardiographic Assessment

4-weeks old Sprague Dawley rats (70-80 g) were anesthetized with intraperitoneal pentobarbital (65 mg/kg) and placed on a ventilator. A suprasternal incision was made exposing the aortic root and a tantalum clip with an internal diameter of 0.58 mm was placed on the ascending aorta. Animals in the sham group underwent a similar procedure without insertion of a clip. In the animals which were aortic-banded we waited 25-30 weeks for the animals to develop left ventricular dilatation and a decrease in ejection fraction by 25% prior to cardiac gene transfer. From the initial 56 who underwent pressure overload hypertrophy only 40 animals survived and were further divided to receive either Ad-shGFP (n=10) or Ad-shPLB (n=10), or rAAV9-shGFP (n=10) or rAAV9-shPLB (n=10). Operators performing the echocardiographic studies were blinded in terms of the animal groups they were studying.

Cardiac Distribution of rAAV9 Vectors After Intravenous Injection

Rats were either transduced with a vector rAAV9-GFP which expresses the marker protein GFP or with saline. 1 month following delivery of rAAV9-GFP or saline the hearts were removed and visualized under a fluorescent system (Maestro *In Vivo* Imaging, Woburn, MA) at 510 nm with single excitation peak at 490 nm of blue light. In addition to this visualization of GFP expression, GFP immunohistological staining was performed 1 month after intravenous (i.v.) injection of rAAV9-GFP to evaluate vector distribution at the microscopic scale.

Experimental Protocol for RNAi Therapy *in vivo*

The adenoviral delivery system has previously been described by our group in detail 17-20. Briefly, after anesthetizing the rats and performing a thoracotomy, a 22 G catheter containing 200 μl of adenoviral (3×10^{10} pfu) solution was advanced from the apex of the left ventricle to the aortic root. The aorta and main pulmonary artery were clamped for 40 sec distal to the site of the catheter and the solution injected, then the chest was closed and the animals were allowed to recover. For experiments with rAAV9, a simple tail vein injection was performed using 5×10^{11} genomes of either rAAV9-shRNA vector. Animals in the sham group were injected with saline.

Hemodynamics and Cardiac Histology during RNAi Therapy

Rats in the different treatment groups and at different stages following adenoviral gene transfer were anesthetized with 40 mg/kg of pentobarbital and mechanically ventilated. A small incision was then made in the apex of the left ventricle and a 2.0 French high fidelity

pressure transducer (MILAR Instruments, TX) introduced into the left ventricle. Pressure measurements were digitized at 1 KHz and stored for further analysis. The operators performing the hemodynamic studies were blinded in terms of the animal groups they were studying.

Statistical Analyses

Data in Fig. 1c-f, 2g, 3a-f and in Suppl. Fig. 1a-e, 3a-e, 4a-c are presented as mean (columns) \pm SD (error bars).

We analyzed the groups of rats intervened on by using a two step procedure. First, we carried out an over-all F test to determine if there is any significant difference existing among any of the means. We then selected two means and calculated Tukey's test for each mean comparison. We then checked to see if Tukey's score is statistically significant with Tukey's probability/critical values.

Statistical significance was accepted at the level of $p < 0.05$.

Statement of Responsibility

The authors had full access to and take full responsibility for the integrity of the data. All authors have read and agree to the manuscript as written.

RESULTS

Optimization of RNA Interference Systems

The determinants of the silencing efficacy of viral RNAi vectors were investigated since we observed that rAAV-shPLB vectors with apparently minor structural differences (Fig. 1a) had grossly different shRNA production rates and target silencing in NRCMs *in vitro* (Fig. 1b,c). For these initial studies in NRCMs the rAAV6 pseudotype was used which has higher transduction efficacy than rAAV9 *in vitro*. For the later RNAi therapeutic investigations reported in Fig. 2 and 3 only rAAV9 was employed which displays superior cardiac transduction *in vivo*. The *in vitro* experiments showed that co-expression of green fluorescent protein (GFP) marker to tag cells harbouring the shPLB vector nearly abolished shPLB production (Fig. 1c) and PLB silencing (Fig. 1b). The presence of a CMV promoter in the expression cassette containing the U6 promoter used for shRNA transcription reduced shRNA production strongly if GFP was driven by the CMV, but also if CMV was linked to a β -intron (Suppl. Fig. 1). Fig. 1 shows that the by far highest efficacy was displayed by an rAAV construct previously considered too short for efficient packaging. Comparison of the shRNA transcription by AdV-shPLB vs rAAV6-shPLB in NRCMs showed a decline to one third by day 10 for the adenoviral, but constant expression for the rAAV vector (Fig. 1c). Ablation of PLB expression at the mRNA level was $> 98\%$ for both vectors at a dose of 4×10^3 p/c. Interestingly, incorporation of a CMV-GFP cassette to allow detection by *in vivo* imaging unexpectedly led to a vector unable to silence its target. CMV promoter-driven marker gene expression is apparently unsuitable for use in U6-shRNA vectors and we therefore choose only the most simple and efficient U6-shRNA vectors (Fig. 1) for *in vivo* RNAi. rAAV9-shRNA was employed for long-term therapy *in vivo* because of its highly

stable shRNA production compared to AdV-shPLB and long-term stability *in vivo*. For short-term therapy the adenoviral vector was used. *In vitro* there was a lag of PLB ablation at the protein level compared to the mRNA level of several days, with protein leveling off at 9 % (AdV-shPLB) and 12 % (rAAV6-shPLB) of baseline, respectively, on day 7 (Fig. 1d). Measurement of $[Ca^{2+}]_i$ transients during AAV9-shPLB treatment of NRCMs (Fig. 1e,f) showed that this vector led to significantly higher amplitude and accelerated transient kinetics (shortened TTP and τ) compared to the AAV9-shGFP group with transients indistinguishable from untreated cells. AdV-shPLB treatment also resulted in a significantly higher amplitude compared to AdV-shGFP. In contrast to the AAV9 groups, TTP was prolonged in AdV-shPLB vs. AdV-shGFP and there was no difference in τ . Studies of sarcoplasmic reticulum (SR) Ca^{2+} loading in the AdV groups showed increased SR Ca^{2+} loading and fractional Ca^{2+} release (FR) from the SR in the AdV-shPLB vs. AdV-shGFP group (Suppl. Fig. 1d). With respect to cell-to-cell variability of transduction *in vitro*, Suppl. Fig. 1b shows grossly homogeneous GFP expression in NRCMs treated with rAAV-GFP marker vector which serves as best possible approximation to a direct demonstration of homogeneous shPLB expression *in vitro*. With current technology the latter cannot be visualized directly since co-expression of GFP together with shPLB extinguishes its silencing capacity (Fig. 1b,c). Homogeneous spatial and temporal distribution of the RNAi vectors in rat hearts *in vivo* is also indirectly inferred by fluorescent imaging (Fig. 2b,c) of a GFP vector of the same type (rAAV9) as used for RNAi therapy (Fig. 3). Fig. 2d and Suppl. Fig. 2a-c show GFP immunohistochemical staining of the heart and other organs after i.v. injection of rAAV9-GFP. Strong and grossly homogeneous expression in the heart contrasts with weak staining of liver and skeletal muscle and no visible staining of the lungs (for quantitation see Suppl. Fig. 2c)

Efficacy of RNA Interference Therapy *in vivo*

Transaortic banding (TAB) led to HF in rats after 30 weeks. The experimental protocol for *in vivo* RNAi therapy is outlined in Fig. 2a. Fluorescent imaging and immunohistological analysis of a GFP vector of the same type (rAAV9) as used for the RNAi therapies showed grossly homogeneous cardiac GFP expression 1 month after i.v. injection at macroscopical and microscopical scale and may be assumed to approximate the cardiac shRNA expression levels generated by the RNAi vectors (Fig. 2b-d). Direct measurement of shPLB production *in vivo* is unfeasible with current technology. Fig. 2f,g show significantly decreased cardiac PLB protein after treatment with either AdV-shPLB or rAAV9-shPLB. SERCA2a protein was decreased in failing hearts, whereas shPLB therapy was accompanied by an increase in cardiac SERCA2a protein. NCX was not significantly changed. Treatment by aortic root injection of AdV-shPLB compared to AdV-shGFP control vector (generating an irrelevant shRNA sequence directed at xenogenic GFP) served as a model of short-term treatment of acute (and potentially reversible) HF. 1 month after injection the left ventricular enddiastolic pressure (LVEDP), rate of LV pressure decrease ($-dp/dt$), and isovolumetric relaxation time constant Tau as measures of diastolic function (Fig. 3a and Suppl. Fig. 3a) were significantly ($p < 0.05$) better in the AdV-shPLB than in the control group. LV systolic pressure (LVSP), rate of LV pressure increase ($+dp/dt$), and the fractional shortening (FS) as parameters of systolic function (Fig. 3b, Suppl. Fig. 3b) were likewise improved. Beyond these beneficial effects on hemodynamics, the massive cardiac hypertrophy and dilation

after TAB were significantly reduced at 1 month (Fig. 3c, Suppl. Fig. 3c). These morphometric data *post mortem* (LV/body weight ratio = LV/BW, LV/tibia length ratio = LV/TL) correlated with echocardiography (Fig. 3d). Histology showed reduced cardiomyocyte size after 1 month of AdvshPLB therapy, whereas cardiac collagen content was unchanged (Fig. 3ef). Survival rates were 8/10 vs. 9/10.

Treatment by i.v. injection of the most efficient rAAV9-shPLB compared to the rAAV9-shGFP vector served as a model of long-term therapy of chronic HF. 3 months after injection diastolic function (LVEDP, $-dp/dt$, Tau) (Fig. 3a, Suppl. Fig. 3a) was significantly improved by rAAV9-shPLB therapy compared to control and no longer significantly different from the sham-operated non-HF group. Systolic function (LVSP, $+dp/dt$, FS) (Fig. 3b, Suppl. Fig. 3b) was also restored, although less so than diastolic functional parameters. Beyond hemodynamics this treatment reduced LV hypertrophy (LV/BW) and dilation (LV/TL) at 3 months (Fig. 3c, Suppl. Fig. 3c). Echocardiography corroborated the reduction of LV wall thickness and dilation (Fig. 3d, Suppl. Fig. 3d). Histology showed reduction of both cardiomyocyte size and cardiac collagen after 3 months of rAAV9-shRNA therapy (Fig. 3ef). Survival of rAAV9-shPLB-treated animals after 3 months was 9/10 vs. 6/10 in the control group.

Cardiac miRNAs and RNA Interference Treatment

shRNAs exploit the cellular machinery of RNAi to mediate therapeutic effects by mimicking the endogenous process, but may disturb cellular miRNA pathways 21. Since miRNAs play important roles in cardiac morphogenesis 12, hypertrophy 13, 14, arrhythmogenesis 15, and failure 16, 22 we searched for possible side-effects of the RNAi vectors at the miRNA level in NRCMs, under standard culture conditions and in the presence of the hypertrophy-inducing drug phenylephrine (PE). In the absence of PE there were no significant effects of any vector on miRNAs 1 or 133. In the presence of PE there was a marked reduction on day 5 which was reversed in NRCMs treated with shPLB vectors. Rat hearts treated with shPLB vector had higher miRNA levels than the shGFP group (Suppl. Fig. 2a-c). With respect to possible side-effects of the RNAi vectors, HE stains of the liver (Fig. 2e) and other organs after vector injection revealed no pathological findings.

DISCUSSION

RNA Interference Therapy of Heart Failure

Building on recent landmark papers by other groups describing highly cardiotropic vector systems 23-26 and after work on rAAV-mediated downregulation of PLB 27-29 the present study demonstrates, for the first time, *in vivo* restoration of cardiac function and reduction of pathological hypertrophy and dilation in a HF animal model. Comparison of the two vector systems used here suggests that for intermediate time scales adenoviral vectors may suffice and even provide advantages over long-term stable rAAV 23-26, since RNAi may be desirable only temporarily in acute and potentially reversible HF. In fact, the significant improvement of diastolic and systolic function and LV morphology 1 month after Adv-shPLB treatment is evidence of an at least functional therapeutic benefit from the adenoviral

system. What has been previously shown for classical gene transfer therapy 18, 19, 20, 30 may obviously work for RNAi-based strategies, too, although there are additional constraints for RNAi vector structure to avoid loss of therapeutic efficacy (Fig. 1a-c) and disturbance of miRNA pathways 21 The experiments further suggest that rAAV-based RNAi may be suitable for the long-term treatment of chronic HF by RNAi strategies. In classical gene therapy studies rAAV vectors have supported stable transgenic protein expression for more than 1 year, which was never achieved with adenoviral systems in immunocompetent hosts. Although shRNA production from rAAVs is in several aspects different from classical gene transfer (Fig. 1), the data from the rAAV arm of our study provide the first evidence that cardiac rAAV9-based shRNA production remains stable for a period of time sufficient for long-term improvement of cardiac function and possibly also survival in HF. We have developed the method for gene delivery by recombinant adenovirus using cross-clamping of the aorta and the pulmonary arteries in rat hearts which yields homogeneous transgene expression 17 and has been used by several groups during the past ten years. In terms of rAAV9, we now show by fluorescent imaging and immunohistochemistry that a single i.v. injection of an rAAV9-GFP marker vector induces strong and grossly homogeneous cardiac GFP expression 1 month after treatment (Fig. 2b-d). The important finding that co-expression of GFP together with shPLB extinguishes its silencing capacity (Fig. 1b,c) prevents, at the present time, direct demonstration of spatial and temporal uniformity of cardiac shRNA synthesis *in vivo* by GFP co-expression. However, uniformity may be deduced by inference from our analogous *in vivo* imaging of GFP expression from adenoviral and rAAV9 vectors. Using rAAV9-GFP we further show that the transduction rate increases over time and reaches 90% at 1 month. Improvement of HF by both RNAi therapeutic protocols is mediated *via* ablation of PLB protein which occurs in cultured NRCMs 10(Fig. 1d) and in rat hearts *in vivo* (Fig. 2f,g). Cardiac PLB protein was significantly decreased following RNAi therapy. Whereas NCX expression was unchanged, SERCA2a expression was more complex. In failing hearts treated with control vectors the SERCA2a expression was decreased as expected in any experimental HF model compared to sham. After RNAi therapy SERCA2a expression was found to be increased compared to HF groups, consistent with the fact that RNAi therapy normalized LV function. Since SERCA2a expression is a well known marker of the degree of HF 31, its increase following RNAi therapy by shPLB reflects the improved status of cardiac function. Both RNAi therapies induced a decrease in cardiomyocyte size (Fig. 3e). In contrast, adenovirus-based therapy over 1 month did not influence the fibrosis induced in failing hearts, whereas long-term rAAV9-based treatment resulted in significantly reduced fibrosis after 3 months (Fig. 3f). This could be a consequence of basic differences between the traditional AdV and the new AAV9 vectors as suggested by the calcium transient studies *in vitro*. AdV *per se* could induce changes in the transcriptional program of target cells different from those of AAV9 (see discussion of possible side-effects below). Irrespective of such differences *in vitro*, however, the effect of the RNAi vectors *in vivo* on PLB ablation, hemodynamics and morphology confirm that the doses chosen for both systems are within the therapeutic range.

The AAV9 vector used in the current study fulfils one first requirement for application in human HF, since it is cardiotropic in primates 29. Beyond its long-term stability, rAAV9 offers further advantages of clinical interest through cardiac targeting after i.v. injection

(Fig. 2*b-d*) and low immunogenicity 32. In contrast to rodents, regulatable PLB modulation is most likely required in humans since permanent PLB deficiency or PLB dysfunction due to genomic mutations has been associated with cardiomyopathies 33-35. Drug-regulatable RNAi appears possible, however, on both vector platforms employed here. Transcriptional control of shRNA expression is technically more demanding than the use of the tissue-specific promoters employed for traditional gene therapy, since these promoters are unable to support proper formation and cleavage of short hairpin RNA. New promoters compatible with shRNA biosynthesis have been developed and may add an additional safety feature to organ-targeted RNAi therapy.

Independent of its therapeutic potential, organ-targeted RNAi may be of use to identify novel gene functions in that organ by functional ablation analogous to classical tissue-specific inducible knockout models. The extent of ablation observed in the current study may suffice to recognize unknown gene functions and the efficacy of this novel analytical approach is likely to increase with the advent of more sophisticated RNAi delivery systems. Importantly, gene ablation by RNAi may be induced at any desired age or disease state and would be more rapid and inexpensive as compared to the traditional models.

Possible Side-Effect of RNA Interference Therapy

The cellular machinery of RNAi evolved over millions of years and is the most efficient and versatile mechanism known for specific gene silencing. shRNAs exploit this machinery to mediate therapeutic effects by mimicking the endogenous process, achieve silencing at far lower concentrations than *antisense* RNAs, but may disturb cellular miRNA pathways 21 and thereby cause hepatotoxicity. When using a cardiotropic rAAV9 serotype with low affinity for the liver we observed no histological evidence of acute or chronic liver damage. We also studied the cardiac-expressed miRNAs 1 and 133 during RNAi treatment. Since malignant arrhythmias are important complications in HF, deregulation of an arrhythmia-related miRNA such as miRNA-1 15 by a novel treatment should be considered as possibly serious adverse effect. None of the RNAi vectors changed miRNA-1 levels in NRCMs, but interestingly shPLB treatment was instead associated with rescue of the miRNA-1 depression induced by PE in these cells and rat hearts on shPLB therapy had higher miRNA levels than controls (Suppl. Fig. 4*a-c*). In conjunction with the trend towards improved survival in the AAV-shPLN treatment group there is thus no evidence of arrhythmogenic side-effects.

Whereas improved contractile function during shPLB therapy results immediately from its influence on excitation-contraction coupling (ECC) *via* the cytoplasmic Ca²⁺ transients, the marked reduction of LV hypertrophy and dilation (Fig. 3*c,d,f*) is not as easily deduced since it involves major reprogramming of the cardiac transcriptome. The RNAi-induced changes of Ca²⁺ homeostasis may affect not only the cytoplasmic Ca²⁺ transients, but also the separate and insulated Ca²⁺ signals generated in the perinuclear space 36-38 which influence transcription. With respect to hypertrophy it is of interest that shPLB treatment was associated with rescue of the PE-induced miRNA-133 depression in NRCMs and higher levels in rat hearts on shPLB treatment (Suppl. Fig. 4*b,c*). The rescue of miRNA-133 which plays a critical role in the control of cardiomyocyte size 13, 14 appears to be linked to RNAi

at the cell level as it also occurs *in vitro* where hemodynamic stress, neurohumoral or cytokine activation as in HF *in vivo* can not play any role.

Whereas our rationale to measure miRNA expression was to test whether shPLB may “poison” the RNAi machinery, differential miRNA induction can also be viewed as “master-switches” that control re-induction of fetal genes during HF 22. A clear distinction between “side-effect” and “master-switch” aspects of miRNA regulation is very difficult and certainly beyond the scope of the current paper. Also clarification of the mechanism by which shPLB-RNAi is linked to the observed changes in miRNA-1 and miRNA-133 (passive association or component of the therapeutic process) requires future studies.

Conclusions

The current study demonstrates, for the first time, high efficacy of a locally targeted RNAi therapeutic strategy in a cardiac disease. Whereas classical gene therapy rests on recombinant protein expression as its basic principle, RNAi therapy employs instead regulatory RNAs with grossly different targeting, kinetics, and toxicity. We provide evidence that under the precondition of careful vector adaptation to the specific requirements of RNAi and if regulatory RNA with high intrinsic activity and target specificity is selected, RNAi therapy may achieve long-term cardiac benefit without apparent toxicity. When using functionally optimized RNAi vectors, and aortic root vector injection or cardiotropic rAAV9 capsids to target RNAi to the heart, there was no evidence of side-effects. Short-term PLB silencing led to improved cardiac function 1 month after aortic root injection of an adenoviral RNAi vector. Long-term RNAi after simple i.v. injection of an optimized rAAV9 vector resulted in restored cardiac function and reduction of cardiac dilation, hypertrophy and fibrosis after a period of 3 months. The rAAV9 approach employs a vector known to target the heart in primates, thus offering potential for clinical translation. Specifically for targets such as PLB where pharmacological approaches have failed so far, the RNAi approach may enhance the therapeutic repertoire for cardiac diseases.

CLINICAL PERSPECTIVE

RNA interference (RNAi) has the potential to be a novel therapeutic strategy in diverse areas of medicine. Whereas gene therapy (already employed for cardiac disorders) rests on recombinant protein expression as its basic principle, RNAi therapy instead employs regulatory RNAs to achieve its effect. Fundamental limitations of chemically synthesized siRNAs to mediate RNAi are their rapid degradation in plasma and target cells, and the unsolved problem of adequate targeting *in vivo*. The present study shows, for the first time, high efficacy of an RNAi therapeutic strategy in a cardiac disease *in vivo*. It demonstrates successful treatment of heart failure (HF) in a rat model by cardiac targeted RNAi ablating phospholamban (PLB), a key regulator of cardiac Ca²⁺ homeostasis. A novel vector was developed based on a cardiotropic adeno-associated virus (rAAV9) which carries RNAi activity to the heart after i.v. injection. Over a period of three months this therapy restored cardiac-function, reversed cardiac dilation and hypertrophy, and reduced cardiac fibrosis. In recent years AAV-based vectors have already overcome key challenges of gene therapy such stability, safety and host immune response. The present study shows now that under the precondition of careful AAV vector adaptation to the

specific requirements of RNAi and if regulatory RNA sequences with high intrinsic activity and target specificity are selected, they may also serve as valuable tools for cardiac RNAi therapy and offer clinical potential. Specifically for targets such as PLB where pharmacological approaches have failed so far, the RNAi approach may enhance the therapeutic repertoire.

Supplementary Material

Refer to Web version on PubMed Central for supplementary material.

Acknowledgments

SOURCES OF FUNDING This work was supported by the *Deutsche Forschungsgemeinschaft* through grant Po 378/6-1 to WP, and through *SFB Transregio 19* projects C5 (WP, HF), C1 (JK, VE), A2 (DW, HS), and Z3 (CT). This study was also supported in part by grants from the *NIH*: R01 HL078691, HL071763, HL080498, and HL083156, a *Leducq Transatlantic Network* (RH), and K01 HL076659 (DL).

Abbreviations

rAAV9	adeno-associated virus pseudotype 9 vector
rAAV9-shGFP (PLB)	rAAV9 generating shRNA to silence GFP (PLB)
AdV	replication-deficient adenovirus 5 vector
AdV-shGFP (PLB)	AdV generating shRNA to silence GFP (PLB)
CMV	cytomegalovirus promoter
FS	fractional shortening
GFP	green fluorescent protein
HF	heart failure
LV	left ventricle
LVSP	LV systolic pressure
LVEDP	LV enddiastolic pressure
miRNA	microRNA
p/c	vector particles per cell
NCX	sodium-calcium-exchanger
PE	phenylephrine
PLB	phospholamban
NRCM	primary neonatal rat cardiac myocyte
RNAi	RNA interference
scAAV	self-complementary AAV
SERCA2a	SR Ca ²⁺ ATPase

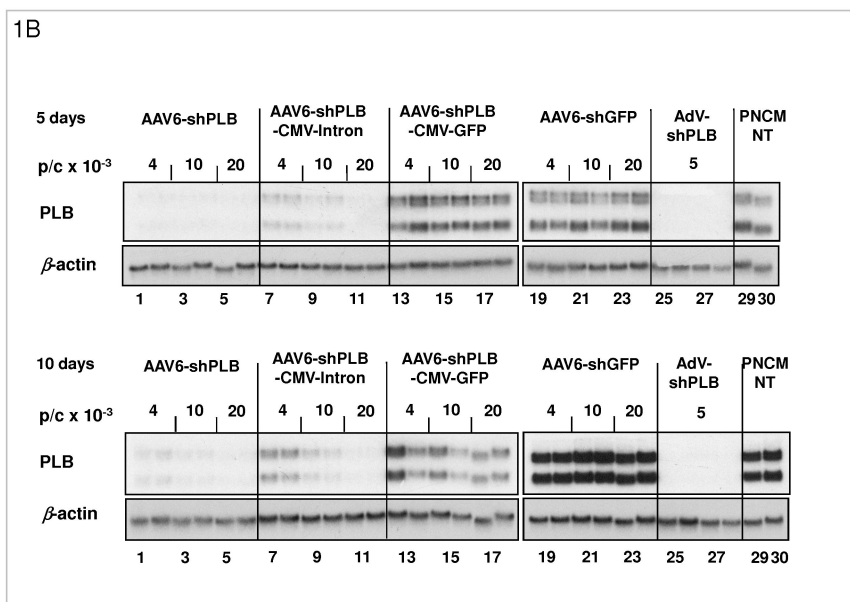
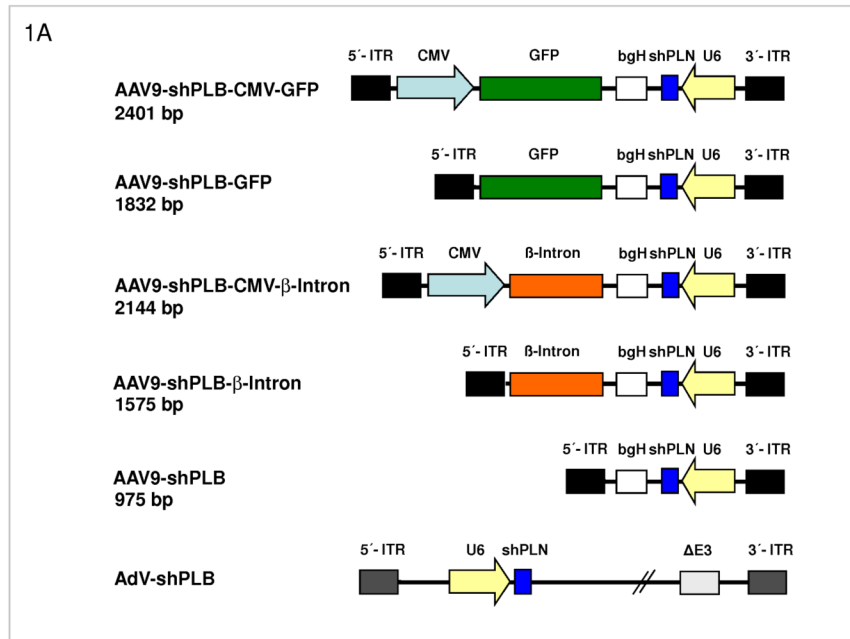
shRNA	short hairpin RNA
SR	sarcoplasmic reticulum
TAB	transaortic banding
Tau	isovolumetric relaxation time constant
τ	time constant of decay of calcium transients
TnI	troponin I
TTP	time to peak of calcium transient

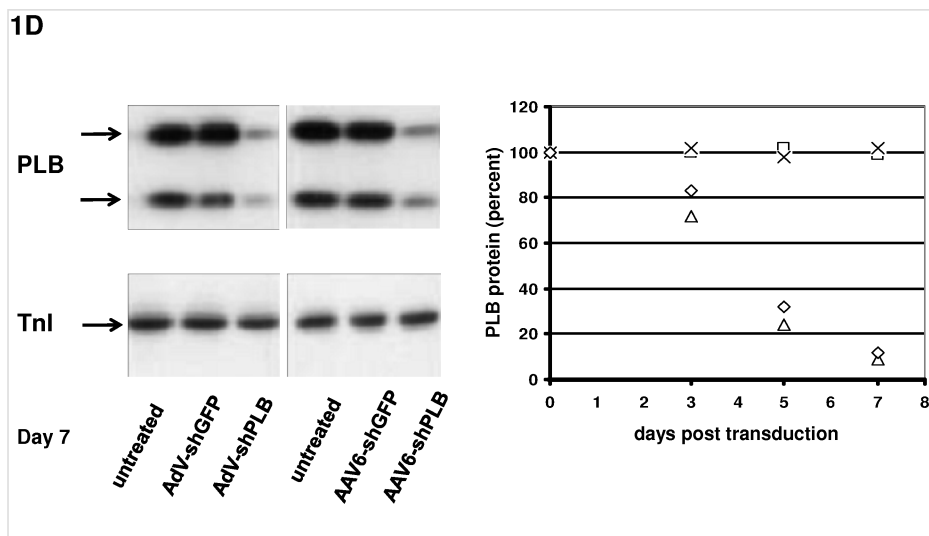
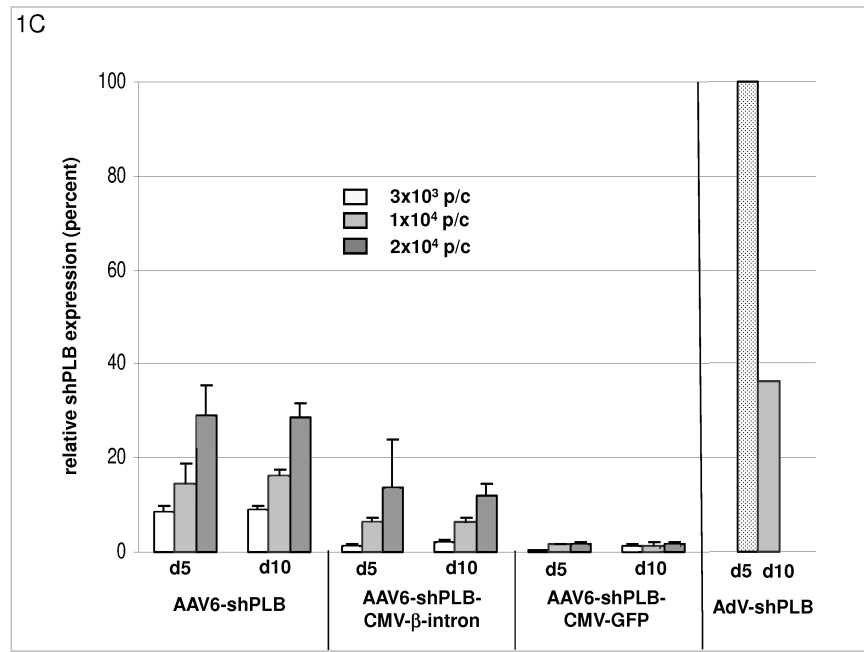
REFERENCES

- Schmidt U, Hajjar RJ, Kim CS, Lebeche D, Doye A, Gwathmey J. Human heart failure: cAMP stimulation of SR Ca²⁺-ATPase activity and phosphorylation level of phospholamban. *Am J Physiol.* 1999; 277:H474–480. [PubMed: 10444471]
- MacLennan D, Kranias E. Phospholamban: A crucial regulator of cardiac contractility. *Nature Reviews Molecular Cell Biology.* 2003; 4:566–576.
- Hoshijima M, Ikeda Y, Iwanaga Y, Minamisawa S, Date M, Gu Y, Iwatate M, Li M, Wang L, Wilson J, Wang Y, Ross J, Chien K. Chronic suppression of heart-failure progression by a pseudophosphorylated mutant of phospholamban via *in vivo* cardiac rAAV gene delivery. *Nature Medicine.* 2002; 8:864–871.
- Iwanaga Y, Hoshijima M, Gu Y, Iwatate M, Dieterle T, Ikeda Y, Date MO, Chrast J, Matsuzaki M, Peterson KL, Chien KR, Ross J Jr. Chronic phospholamban inhibition prevents progressive cardiac dysfunction and pathological remodeling after infarction in rats. *J Clin Invest.* 2004; 113:727–736. [PubMed: 14991071]
- Eizema K, Fechner H, Bezstarosti K, Schneider-Rasp S, van der Laarse A, Wang H, Schultheiss H-P, Poller W, Lamers J. Adenovirus-based phospholamban-antisense-mRNA expression as a novel approach to improve cardiac contractile dysfunction - Comparison of a constitutive viral versus an endothelin-1-responsive cardiac promoter. *Circulation.* 2000; 101:2193–2199. [PubMed: 10801761]
- Dieterle T, Meyer M, Gu Y, Belke DD, Swanson E, Iwatate M, Hollander J, Peterson KL, Ross J Jr, Dillmann WH. Gene transfer of a phospholamban-targeted antibody improves calcium handling and cardiac function in heart failure. *Cardiovasc Res.* 2005; 67:678–688. [PubMed: 15927173]
- Meyer M, Belke DD, Trost SU, Swanson E, Dieterle T, Scott B, Cary SP, Ho P, Bluhm WF, McDonough PM, Silverman GJ, Dillmann WH. A recombinant antibody increases cardiac contractility by mimicking phospholamban phosphorylation. *Faseb J.* 2004; 18:1312–1314. [PubMed: 15180962]
- Minamisawa S, Hoshijima M, Chu G, Ward C, Frank K, Gu Y, Martone M, Wang Y, Ross J, Kranias E, Giles W, Chien K. Genetic complementation identifies chronic phospholamban-sarcoplasmic reticulum calcium ATPase interaction as a critical calcium cycling defect in the progression of dilated cardiomyopathy. *Cell.* 1999; 99:313–322. [PubMed: 10555147]
- Watanabe A, Arai M, Yamazaki M, Koitabashi N, Wuytack F, Kurabayashi M. Phospholamban ablation by RNA interference increases Ca²⁺ uptake into rat cardiac myocyte sarcoplasmic reticulum. *J Mol Cell Cardiol.* 2004; 37:691–698. [PubMed: 15350842]
- Fechner H, Suckau L, Kurreck J, Sipo I, Wang X, Pinkert S, Loschen S, Rekitke J, Weger S, Dekkers D, Vetter R, Erdmann V, Schultheiss H-P, Paul M, Lamers J, Poller W. Highly efficient and specific modulation of cardiac calcium homeostasis by adenovector-derived short hairpin RNA targeting phospholamban. *Gene Therapy.* 2007; 14:211–218. [PubMed: 17024101]
- Zolotukhin S, Byrne BJ, Mason E, Zolotukhin I, Potter M, Chesnut K, Summerford C, Samulski R, Muzyczka N. Recombinant adeno-associated virus purification using novel methods improves infectious titer and yield. *Gene Ther.* 1999; 6:973–985. [PubMed: 10455399]

12. Zhao Y, Ransom JF, Li A, Vedantham V, von Drehle M, Muth A, Tsuchihashi T, McManus M, Schwartz R, Srivastava D. Dysregulation of Cardiogenesis, Cardiac Conduction, and Cell Cycle in Mice Lacking miRNA-1-2. *Cell*. 2007; 129:303–317. [PubMed: 17397913]
13. Care A, Catalucci D, Felicetti F, Bonci D, Addario A, Gallo P, Bang ML, Segnalini P, Gu Y, Dalton N, Elia L, Latronico M, Hoydal M, Autore C, Russo MA, Dorn G 2nd, Ellingsen O, Ruiz-Lozano P, Peterson K, Croce C, Peschle C, Condorelli G. MicroRNA-133 controls cardiac hypertrophy. *Nat Med*. 2007; 13:613–618. [PubMed: 17468766]
14. van Rooij E, Sutherland L, Qi X, Richardson J, Hill J, Olson E. Control of stress-dependent cardiac growth and gene expression by a MicroRNA. *Science*. 2007; 316:575–579. [PubMed: 17379774]
15. Yang B, Lin H, Xiao J, Lu Y, Luo X, Li B, Zhang Y, Xu C, Bai Y, Wang H, Chen G, Wang Z. The muscle-specific microRNA miR-1 regulates cardiac arrhythmogenic potential by targeting GJA1 and KCNJ2. *Nat Med*. 2007; 13:486–491. [PubMed: 17401374]
16. van Rooij E, Sutherland L, Liu N, Williams A, McAnally J, Gerard R, Richardson J, Olson E. A signature pattern of stress-responsive microRNAs that can evoke cardiac hypertrophy and heart failure. *Proc Natl Acad Sci U S A*. 2006; 103:18255–18260. [PubMed: 17108080]
17. Hajjar R, Schmidt U, Matsui T, Guerrero J, Lee K-H, Gwathmey J, Dec G, Semigran M, Rosenzweig A. Modulation of ventricular function through gene transfer *in vivo*. *Proceedings of the National Academy of Science USA*. 1998; 95:5251–5256.
18. del Monte F, Lebeche D, Guerrero JL, Tsuji T, Doye AA, Gwathmey JK, Hajjar RJ. Abrogation of ventricular arrhythmias in a model of ischemia and reperfusion by targeting myocardial calcium cycling. *Proc Natl Acad Sci U S A*. 2004; 101:5622–5627. [PubMed: 15044708]
19. Sakata S, Lebeche D, Sakata N, Sakata Y, Chemaly ER, Liang LF, Tsuji T, Takewa Y, Del Monte F, Peluso R, Zsebo K, Jeong D, Park WJ, Kawase Y, Hajjar R. Restoration of mechanical and energetic function in failing aortic-banded rat hearts by gene transfer of calcium cycling proteins. *J Mol Cell Cardiol*. 2007; 42:852–861. [PubMed: 17300800]
20. Sakata S, Lebeche D, Sakata Y, Sakata N, Chemaly ER, Liang L, Nakajima-Takenaka C, Tsuji T, Konishi N, del Monte F, Hajjar RJ, Takaki M. Transcoronary gene transfer of SERCA2a increases coronary blood flow and decreases cardiomyocyte size in a type 2 diabetic rat model. *Am J Physiol Heart Circ Physiol*. 2007; 292:H1204–1207. [PubMed: 17012346]
21. Grimm D, Streetz KL, Jopling CL, Storm TA, Pandey K, Davis CR, Marion P, Salazar F, Kay MA. Fatality in mice due to oversaturation of cellular microRNA/short hairpin RNA pathways. *Nature*. 2006; 441:537–541. [PubMed: 16724069]
22. Thum T, Galuppo P, Wolf C, Fiedler J, Kneitz S, van Laake L, Doevendans P, Mummery C, Borlak J, Haverich A, Gross C, Engelhardt S, Ertl G, Bauersachs J. MicroRNAs in the human heart: a clue to fetal gene reprogramming in heart failure. *Circulation*. 2007; 116:258–267. [PubMed: 17606841]
23. Wang Z, Zhu T, Qiao C, Zhou L, Wang B, Zhang J, Chen C, Li J, Xiao X. Adeno-associated virus serotype 8 efficiently delivers genes to muscle and heart. *Nat Biotechnol*. 2005; 23:321–328. [PubMed: 15735640]
24. Gregorevi P, Blankinship M, Allen J, Crawford R, Meuse L, Miller D, Russell D, Chamberlain J. Systemic delivery of genes to striated muscles using adeno-associated viral vectors. *Nature Medicine*. 2004; 10:828–834.
25. Inagaki K, Fuess S, Storm T, Gibson G, McTiernan C, Kay M, Nakai H. Robust systemic transduction with AAV9 vectors in mice: efficient global cardiac gene transfer superior to that of AAV8. *Mol Ther*. 2006; 14:45–53. [PubMed: 16713360]
26. Paak C, Mah C, Thattaliyath B, Conlon T, Lewis M, Cloutier D, Zolotukhin I, Tarantal A, Byrne B. Recombinant adeno-associated virus serotype 9 leads to preferential cardiac transduction *in vivo*. *Circ Res*. 2006; 99:e3–9. [PubMed: 16873720]
27. Andino LM, Takeda M, Kasahara H, Jakymiw A, Byrne B, Lewin A. AAV-mediated knockdown of phospholamban leads to improved contractility and calcium handling in cardiomyocytes. *J Gene Med*. 2008; 10:132–142. [PubMed: 18064719]
28. Li J, Hu SJ, Sun J, Zhu ZH, Zheng X, Wang GZ, Yao YM, Chen NY, Zhao XY. Construction of phospholamban antisense RNA recombinant adeno-associated virus vector and its effects in rat cardiomyocytes. *Acta Pharmacol Sin*. Jan; 2005 26(1):51–55. [PubMed: 15659114]

29. Champion HC, Georgakopoulos D, Haldar S, Wang L, Wang Y, Kass D. Robust adenoviral and adeno-associated viral gene transfer to the in vivo murine heart: application to study of phospholamban physiology. *Circulation*. 2003; 108:2790–2797. [PubMed: 14638552]
30. Sakata S, Lebeche D, Sakata Y, Sakata N, Chemaly ER, Liang LF, Padmanabhan P, Konishi N, Takaki M, del Monte F, Hajjar R. Mechanical and metabolic rescue in a type II diabetes model of cardiomyopathy by targeted gene transfer. *Mol Ther*. 2006; 13:987–996. [PubMed: 16503203]
31. Lowes B, Gilbert E, Abraham W, Minobe WA, Larrabee P, Ferguson D, Wolfel E, Lindenfeld J, Tsvetkova T, Robertson A, Quaife R, Bristow M. Myocardial gene expression in dilated cardiomyopathy treated with β -blocking agents. *N Engl J Med*. 2002; 346:1357–1365. [PubMed: 11986409]
32. Ding Z, Georgiev P, Thöny B. Administration-route and gender-independent long-term therapeutic correction of phenylketonuria (PKU) in a mouse model by recombinant adeno-associated virus 8 pseudotyped vector-mediated gene transfer. *Gene Ther*. 2006; 13:587–593. [PubMed: 16319947]
33. Schmitt J, Kamisago M, Asahi M, Li G, Ahmad F, Mende U, Kranias E, MacLennan D, Seidman J, Seidman C. Dilated Cardiomyopathy and Heart Failure Caused by a Mutation in Phospholamban. *Science*. 2003; 299:1410–1413. [PubMed: 12610310]
34. Haghghi K, Kolokathis F, Gramolini AO, Waggoner JR, Pater L, Lynch R, Fan G, Tsiapras D, Parekh R, Dorn G 2nd, MacLennan D, Kremastinos D, Kranias E. A mutation in the human phospholamban gene, deleting arginine 14, results in lethal, hereditary cardiomyopathy. *Proc Natl Acad Sci U S A*. 2006; 103:1388–1393. [PubMed: 16432188]
35. Zhao W, Yuan Q, Qian J, Waggoner JR, Pathak A, Chu G, Mitton B, Sun X, Jin J, Braz J, Hahn H, Marreez Y, Syed F, Pollesello P, Annala A, Wang H, Schultz Jel J, Molkenin J, Liggett S, Dorn G 2nd, Kranias E. The presence of Lys27 instead of Asn27 in human phospholamban promotes sarcoplasmic reticulum Ca^{2+} -ATPase superinhibition and cardiac remodeling. *Circulation*. 2006; 113:995–1004. [PubMed: 16476846]
36. Wu X, Zhang T, Bossuyt J, Li X, McKinsey T, Dedman J, Olson E, Chen J, Brown J, Bers D. Local InsP_3 -dependent perinuclear Ca^{2+} signaling in cardiac myocyte excitation-transcription coupling. *J Clin Invest*. 2006; 116:675–682. [PubMed: 16511602]
37. Molkenin J. Dichotomy of Ca^{2+} in the heart: contraction versus intracellular signaling. *J Clin Invest*. 2006; 116:623–626. [PubMed: 16511595]
38. Kockskämper J, Seidlmayer L, Walther S, Hellenkamp K, Maier L, Pieske B. Endothelin-1 enhances nuclear Ca^{2+} transients in atrial myocytes through $\text{Ins}(1,4,5)\text{P}_3$ -dependent Ca^{2+} release from perinuclear Ca^{2+} stores. *Journal of Cell Science*. 2008; 121:186–195. [PubMed: 18089647]





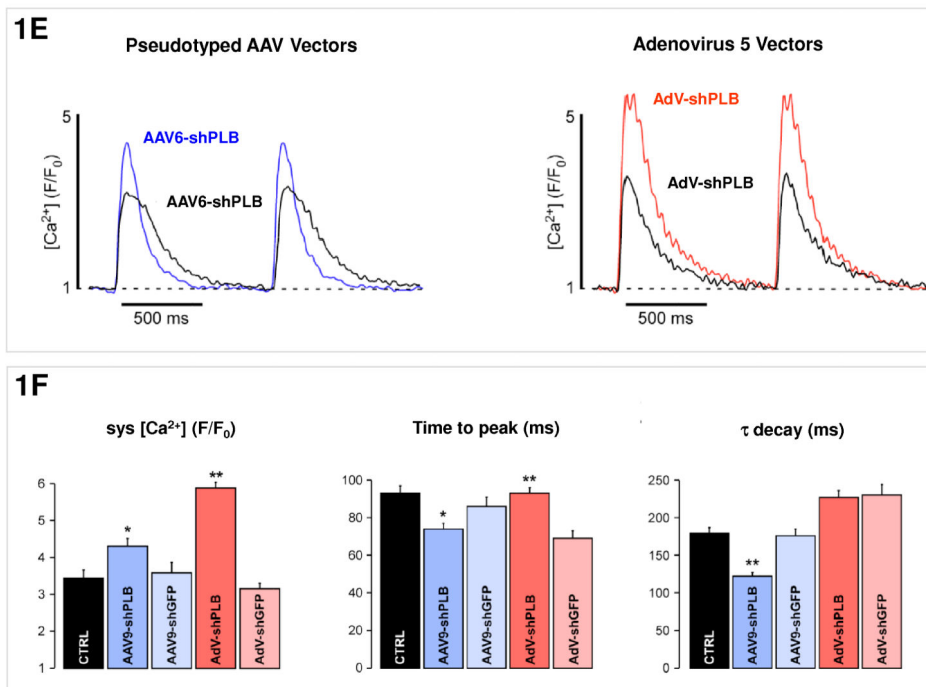


Fig. 1. RNAi Vectors for HF Therapy

A: Maps of the RNAi vector genomes. Self-complementary “dimeric” AAV genomes (rAAV2) were pseudotyped into rAAV6 or rAAV9 capsids for studies in cardiomyocytes *in vitro* or HF rats *in vivo*, respectively. rAAV-shPLB has the same U6-shRNA transcription system as AdV-shPLB and the corresponding shGFP control vectors. Two further rAAV vectors carried CMV-GFP or CMV-β-intron expression cassettes in head-to-head orientation with the U6-shPLB sequence and separated from them by a bovine growth hormone (bgH) terminal signal. To assess the influence of the CMV promoter on vector function the CMV-free variants rAAV-shPLB-GFP and rAAV-shPLB-β-intron were constructed. Please note that the genomes in the rAAV6 vectors for *in vitro* work are identical to those shown for the rAAV9 vectors shown here.

B: Comparison of the target silencing efficacy of shRNA vectors in NRCMs. Cells were harvested 5 (upper part) or 10 days (lower part), respectively, after treatment with the respective vector at the dose in particles per cell (p/c) given above the lanes. Northern blots were then carried out using a rat PLB-specific probe. To confirm equal RNA loading the blots were striped and rehybridized with a β-actin-specific probe. Lanes 1 to 18 show dose dependency of RNAi-mediated PLB-mRNA downregulation for the rAAV-based vectors rAAV-shPLB (lane 1-6), rAAV-shPLB-CMV-β-intron (lane 7-12), and rAAV-shPLB-CMV-GFP (lane 13-18). Lanes 19-24 show as a control for unspecific shRNA effects PLB-mRNA expression after treatment with rAAV-shGFP which generates an shRNA sequence targeting GFP (lanes 19-24). There was no difference towards untreated cells (lanes 29,30). For comparison with rAAV the adenovector AdV-shPLB (lanes 25-28) was used. PLB-mRNA was 98% ablated until day 10 by rAAV-shPLB at the lowest dose of 4×10^3 p/c (lanes 1,2), similar to AdV-shPLB (lanes 25-28). Incorporation of a CMV-GFP expression cassette in the rAAV-shPLB vector (lanes 7-12) to provide this vector with a tag which is

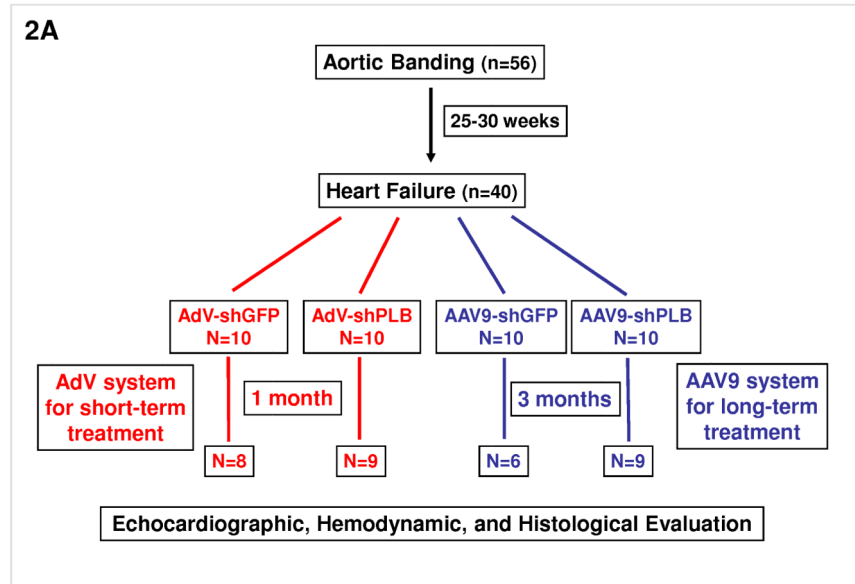
easily detectable by *in vivo* imaging, led to strong GFP expression in infected cells (not shown) but unexpectedly abolished its PLB gene silencing effect. Incorporation of a CMV- β -intron cassette (lanes 12-18) had a similar but less pronounced effect. We therefore used only rAAV9-shPLB vs rAAV9-shGFP and AdV-shPLB vs AdV-shGFP for *in vivo* therapy (Fig. 2a-g and 3a-f).

C: The cellular shRNA levels produced by the vectors from panel B. In the presence of a CMV-GFP cassette shPLB production was abolished (lanes 13-18), whereas the U6-shPLB vector without additional sequences showed stable expression over 5 (lanes 1-3) and 10 days (lanes 4-6). AdV-shPLB generated very high shPLB levels on day 5 which then declined rather rapidly in NRCMs. Studies with further vectors (Suppl. Fig. 1a-c) showed that interaction of the CMV promoter with the shRNA-transcribing polymerase type III U6 promoter apparently disturbs shRNA transcription from the respective AAV vectors.

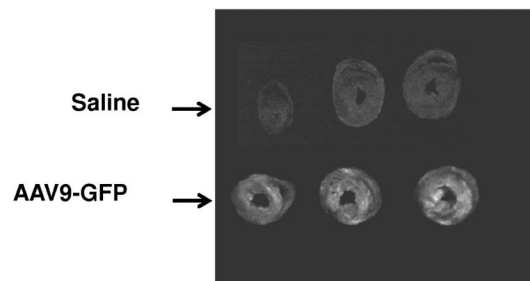
D: On the left a Western blot analysis of PLB protein during treatment of NRCMs and on the right its quantitation on days 3, 5, and 7 after vector addition is shown. AdV-shPLB and rAAV6-shPLB resulted on day 7 in downregulation of cellular PLB to 9 % and 13 %, respectively, of baseline.

E: $[Ca^{2+}]_i$ transients in NRCMs during AAV9-shPLB treatment showed significantly higher amplitudes and accelerated transient kinetics (shortened TTP and τ) compared to the AAV9-shGFP group with transients indistinguishable from untreated cells. AdV-shPLB treatment also resulted in a significantly higher amplitude than in AdV-shGFP controls. In contrast to the AAV9 groups, TTP was prolonged in the AdV-shPLB vs. AdV-shGFP group which displayed no difference in τ .

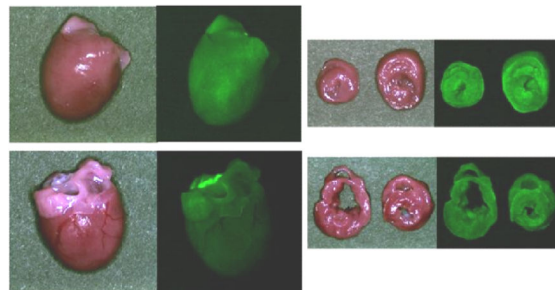
F: Statistical evaluation of the $[Ca^{2+}]_i$ transients. * denotes $p < 0.05$ and ** $p < 0.01$. Additional studies of sarcoplasmic reticulum (SR) Ca^{2+} loading in the adenovirus groups (measured by rapid caffeine addition) were performed (Suppl. Fig. 1d,e) and showed increased SR Ca^{2+} loading and fractional Ca^{2+} release from the SR in AdV-shPLB vs. AdV-shGFP group.



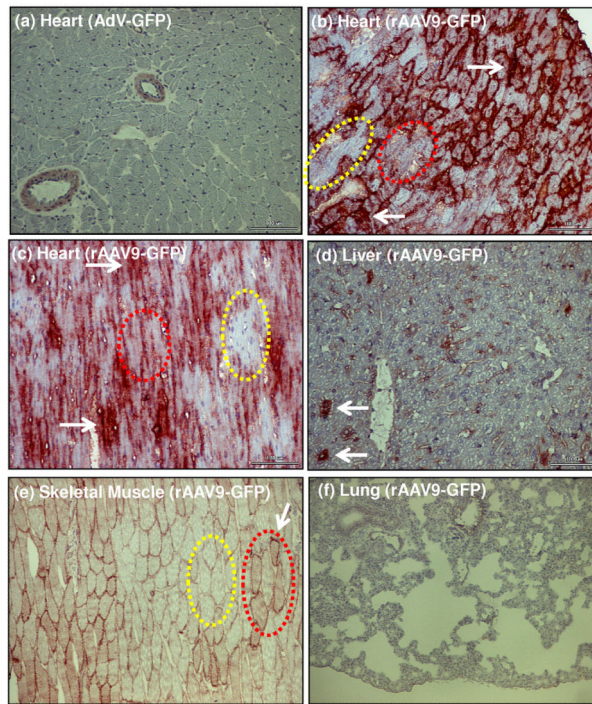
2B



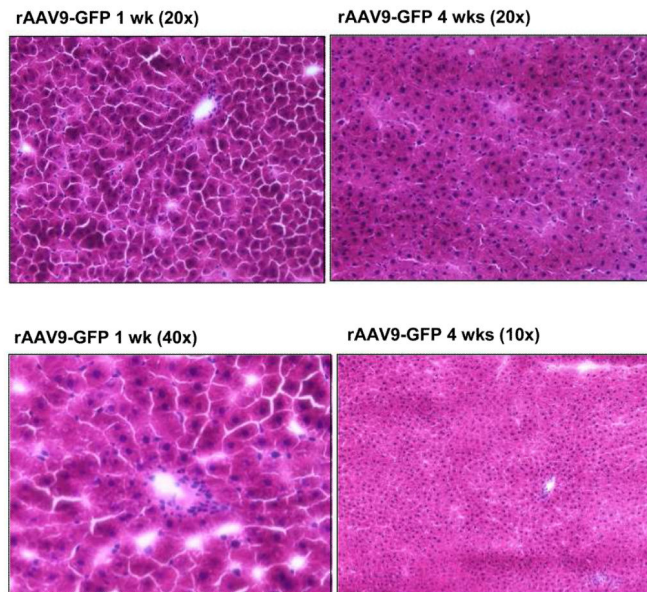
2C



2D



2E



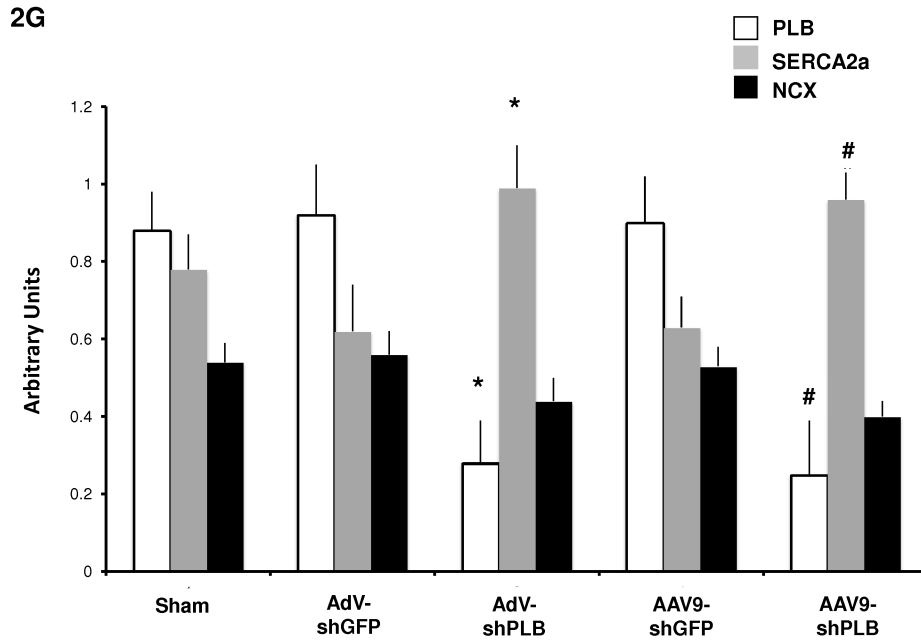
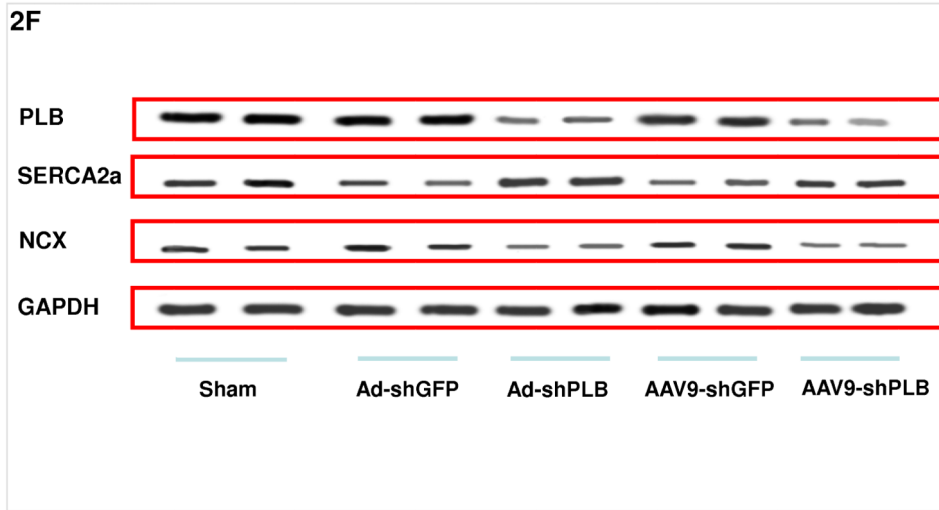


Fig. 2. Protocol for RNAi Therapy of HF

A: Animals for the *in vivo* RNAi therapy study were divided in two groups: one of 56 animals with aortic banding (TAB) and a second of 12 sham-operated. In the TAB animals we waited 25-30 weeks for them to develop LV dilatation and a decrease in fractional shortening by 25% (echocardiography) prior to cardiac RNAi vector transfer. From 56 TAB animals 40 survived and were further divided to receive Adv-shGFP (n=10), Adv-shPLB (n=10), rAAV9-shGFP (n=10), or rAAV9-shPLB (n=10). 3×10^{10} pfu of each Adv were injected in 200 μ l of solution. For experiments with rAAV9, tail vein injection was done using 5×10^{11} genomes of either vector. Outcome evaluation by echocardiography, tip catheter, morphometry, and histology was after 1 month in the Adv and after 3 months in the rAAV9 groups (Fig. 3a-f). In the Adv groups 8/10 and 9/10 animals survived after 1

month. After 3 months 9/10 survived in the rAAV-shPLB and 6/10 in the rAAV-shGFP group.

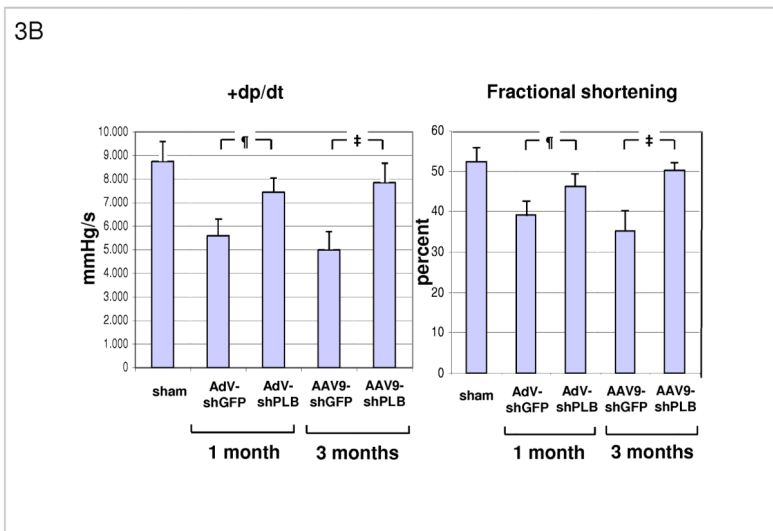
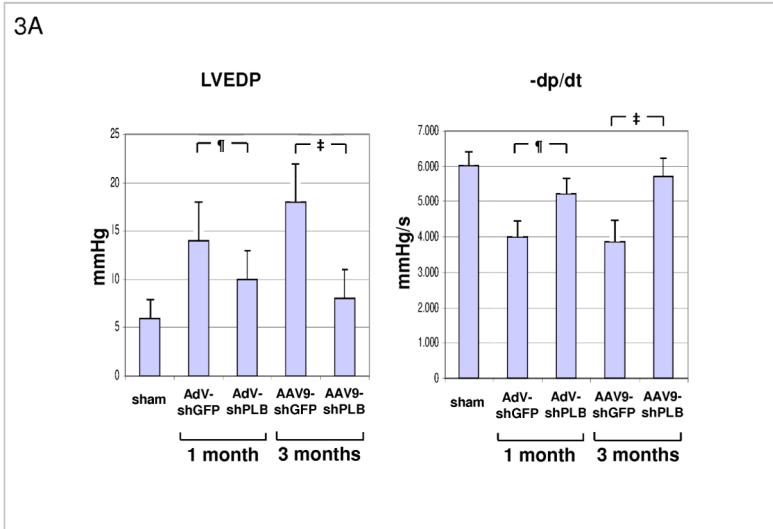
B: Rats were injected i.v. with an rAAV9-GFP vector expressing green fluorescent protein, or with saline. 1 month later the hearts were removed and visualized by GFP imaging which showed a grossly homogeneous signal in cardiac cross sections in the (lower) rAAV9-GFP group, and no signal in the (upper) saline group. **C:** An overview on GFP fluorescence from hearts from rAAV9-GFP-treated rats reaching 90% of surface area at 1 month.

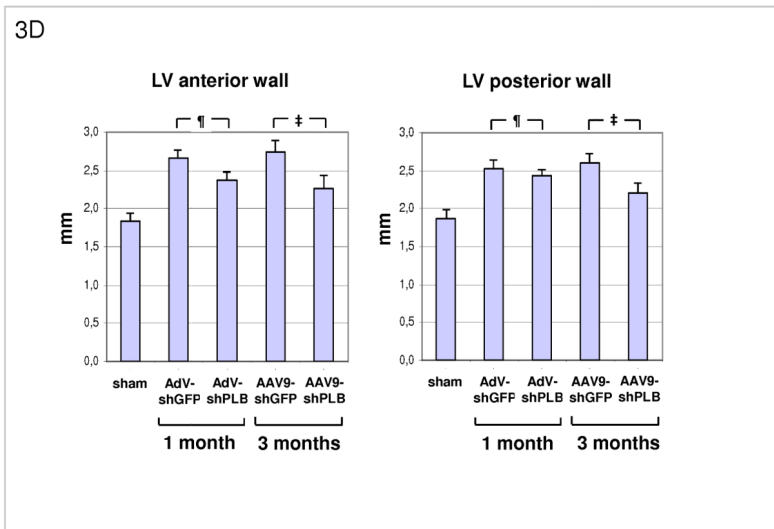
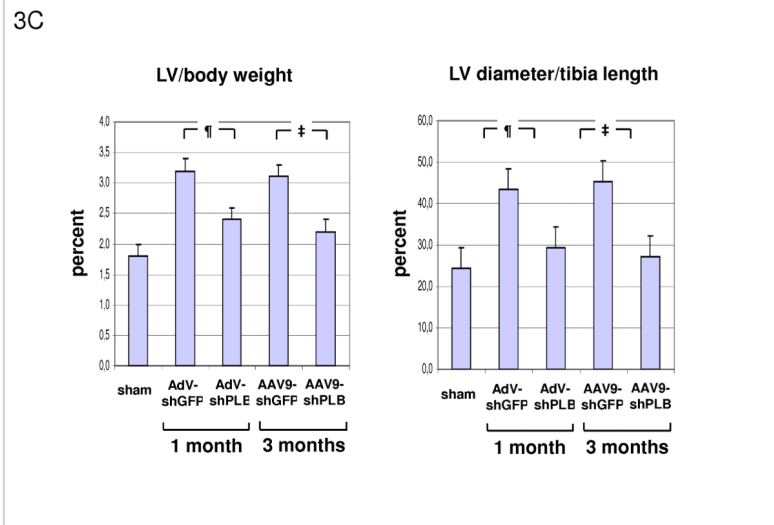
D: Immunohistochemical staining of GFP in different organs 1 month after i.v. injection of rAAV9-GFP. Whereas after i.v. injection of an adenoviral vector (AdV-GFP) no GFP was detected in the heart (a), rAAV9-GFP treatment resulted in strong GFP expression (b)(c) which was grossly homogeneous. Few areas are completely devoid of GFP immunoreactivity (encircled yellow), others show homogeneous cytoplasmic staining (encircled red). Staining is particularly dense at sites where high expression over 1 month has obviously resulted in the formation of precipitates (white arrows) of GFP which is stable in cells, in contrast to shRNA generated from RNAi vectors. An average of 70% of cardiomyocytes were positive by immunohistochemistry, with variability of expression among individual cells. (e) shows skeletal muscle with faint staining of a fraction of cells, whereas the liver shows prominent signal of individual cells only (d). No signal was visible in the lungs. Further data on AAV9 distribution are given in Suppl. Fig. 2c with GFP quantitation by Western blot analyses, documenting highest affinity of rAAV9-GFP expression for the heart. Liver and skeletal muscle showed low and the lungs only very faint expression. Suppl. Fig. 2ab document specificity of the GFP staining.

E: Haematoxylin-eosin staining of livers 1 week and 4 weeks after i.v. injection of rAAV9-GFP shows no evidence of toxicity. rAAV-shRNA vector also resulted in no hepatotoxicity.

F: Representative Western blots showing a significant decrease of cardiac PLB protein after 1 month of AdV-shPLB and 3 months of rAAV9-shPLB therapy compared to the shGFP control groups. The NCX and GAPDH protein remained unchanged. SERCA2a was decreased in the shGFP groups which were in heart failure as compared to sham, whereas SERCA2a was significantly increased in both shPLB groups.

G: Statistical evaluation of Western blots from the different treatment groups. * denotes $p < 0.05$ compared to AdV-shGFP, # $p < 0.05$ compared to rAAV9-shGFP.





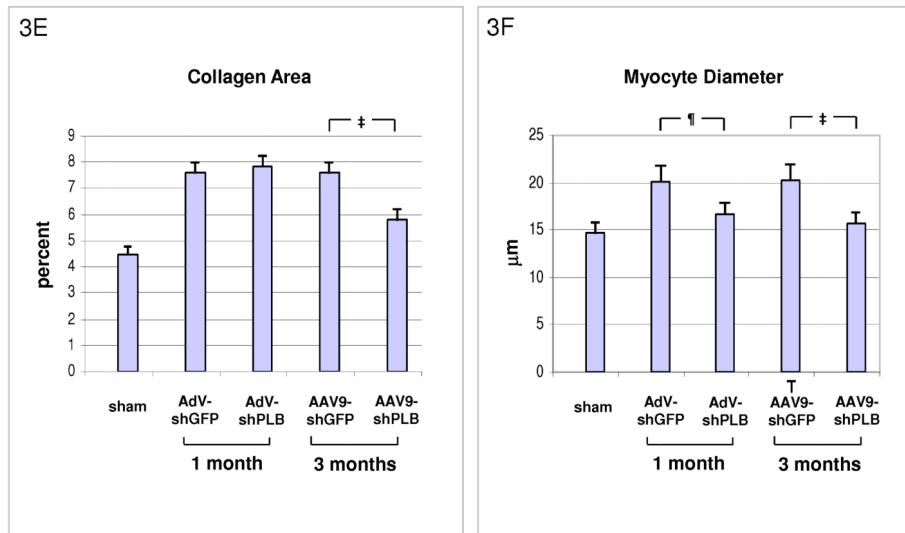


Fig. 3. Functional and Morphological Effects of RNAi Therapy

A: Influence of RNAi treatments on parameters of diastolic LV function. The high LV filling pressure (LVEDP) in rats after TAB was significantly lowered by shPLB vectors (lanes 3,5) compared to shGFP controls (lanes 2,4). The maximal rate of pressure fall ($-dP/dt$) was significantly increased by shPLB treatment, also the isovolumetric relaxation time constant Tau (Suppl. Fig. 3a). Values were restored to normal range (lane 1) after 3 months of rAAV-shPLB therapy (lane 5).

¶ denotes $p < 0.05$ for AdV-shPLB vs. AdV-shGFP, ‡ $p < 0.05$ for rAAV9-shPLB vs. rAAV9-shGFP.

B: RNAi treatment effects on systolic function. Echocardiography showed normalized fraction shortening (FS) after 3 months of rAAV-shPLB therapy, whereas FS improvement was also significant but less pronounced for AdV-shPLB. The maximal rate of pressure rise ($+dP/dt$) was improved compared to controls, also the systolic pressure (LVSP)(Suppl. Fig. 3b).

C: Morphometry *post mortem* showing marked LV hypertrophy induced by TAB (lanes 2,4) with LV weight (Suppl. Fig. 3c) and LV/body weight (LV/BW) ratio $\approx 2/3$ thirds above baseline (lane 1). There was also marked LV dilation (LV diameter/tibia length ratio). The latter was reduced to within the normal range after 1 or 3 months of therapy with AdV-shPLB or rAAV9-shPLB (lanes 3,5). Cardiac hypertrophy was significantly reduced by both vector types.

D: A summary of echocardiographic data on cardiac morphology which corroborate the morphometric findings in panel C (see also Suppl. Fig. 3d).

E: Cardiac collagen content in HF animals after RNAi therapy. After therapy with AdV-shPLB there was no decrease in fibrosis at 1 month, whereas rAAV9-shRNA treatment resulted in significantly reduced fibrosis at 3 months. The control vectors had no effect.

F: Both treatment modes induced a significant decrease in cardiomyocyte diameters.